CANADIAN JOURNAL OF EXPLORATION GEOPHYSICS
VOL. 24, NO. 2 (DECEMBER 1988), P. 117-123

ZERO-OFFSET REFLECTION MODELLING WITH SPATIAL WAVELETS

ATUL NAUTIYAL[1]

ABSTRACT

Modelling of the two-dimensional zero-offset seismic compressional-wave field can be performed as a one-dimensional spatial convolution in the space-frequency domain. This article provides a brief review of this technique, called the spatial-wavelet method.

Illustrative examples use elementary earth models with media of varying complexity: constant velocity, horizontally stratified velocities and laterally varying velocities. The spatial wavelet is formulated for a constant-velocity medium and modelling in such a case is straightforward. For horizontally stratified velocities there is no formulation for the spatial wavelet and in practical application discrete layers with constant velocities have been considered. In each layer the constant-velocity formulation was used. Lateral velocity changes were tackled by using adaptive spatial wavelets which were governed by the lateral velocity profile.

The modelling results indicate that the method was successful in the constant and horizontally stratified velocity cases, but the attempt with the laterally varying velocity model suggests that further work can be done.

INTRODUCTION

Computer modelling of seismic reflection data with the acoustic wave equation is an area of active and intensive research. Some examples of such work are Tieman (1980) who used a space-time finite-difference method; Kosloff and Baysal (1982) who developed a Fourier method; Carter and Frazer (1983) who used a Kirchhoff integral technique; Kelamis and Kjartansson (1985) who presented a space-frequency version of the finite-difference method; and Shtivelman (1985) who investigated a hybrid method using analytical and numerical techniques. Less frequently discussed is the spatial wavelet method developed by Berkhout (1982, 1984). Although Berkhout's works are primarily concerned with migration, the principles of modelling are also developed there. An important characteristic of this method is that the wave-field continuation procedure can be implemented as a convolution. Most geophysicists are familiar with convolution, and therefore it offers an appealing method for understanding the fundamentals of modelling and migration. (Whether the technique is the most efficient or accurate is another matter.) In this paper I give a short review of the spatial-wavelet technique for modelling and investigate its application to elementary earth models with varying degrees of complexity in the velocity structure. This is done with a professional readership in mind and, for this reason, mathematical details are omitted. However, the introductory material in this paper should help readers prepare for investigating the more mathematical work of Berkhout (1982, 1984) and other wave-equation modelling/migration methods (e.g., finite-difference, finite-element and Fourier) which, in my opinion, are more difficult to appreciate physically.

CONVOLUTION WITH SPATIAL WAVELETS

An important result from scalar diffraction theory for monochromatic (single-frequency) waves is that one-way propagation may be cast as a convolutional process over the space domain (e.g., Born and Wolf, 1975; Berkhout, 1982, 1984). For most geometries this can be expressed in terms of the monochromatic Kirchhoff-Helmholtz integral. Assuming that the source and recording surfaces are planar gives a variant of the Kirchhoff-Helmholtz integral known as the Rayleigh-Sommerfeld integral. A further simplification assumes two-dimensional (2-D) geometry so that all earth properties are considered invariant along one of the space coordinates. The result is that the propagation may be expressed by a one-dimensional (1-D) convolution

$$P(x_o, z_{i+1}, f_n) = \int_x W(x_o - x, \Delta z, f_n)\, P(x, z_i, f_n)\, dx. \quad (1)$$

The quantity P represents the wave field, x_o indicates the receiver location on the recording plane at a depth level z_{i+1}, x indicates the location of emitters on the source surface at a depth level z_i and f_n is the nth frequency component. Convolution over space must be done for each frequency when the wave field is composed of many frequencies. If a

Manuscript received by the Editor July 21, 1988; revised manuscript received October 19, 1988.

[1]Formerly, Department of Geophysics and Astronomy, University of British Columbia, Vancouver, B.C. V6T 1W5; presently, Amoco Canada Petroleum Co., Ltd., Amoco Centre, 240 4th Avenue S.W., Calgary, Alberta T2P 2H8

The author wishes to thank D.T. Easley and T. Thing for initial reviews, T.E. Scheuer for the use of his migration programs and R.J. Brown and the Journal reviewers for their helpful comments. Amoco Canada generously provided facilities for the preparation of this paper. This work was partly sponsored by grant A4270 to D.W. Oldenburg from the Natural Sciences and Engineering Research Council.

monochromatic point source of unit amplitude at $x = 0$ generates the wave field at depth z_i, then the response at depth z_{i+1} is given by $W(x, \Delta z, f_n)$. Therefore, $W(x, \Delta z, f_n)$ is the spatial impulse response or the spatial wavelet for the temporal frequency f_n and extrapolation step $\Delta z = z_{i+1} - z_i$. For a homogeneous medium the spatial wavelet is a complex-valued symmetric function about the point source. The 2-D spatial wavelet for the one-way wave equation is given by

$$W(x) = -\frac{ik\Delta z}{2}\frac{H_1^{(2)}\left(k\sqrt{x^2+\Delta z^2}\right)}{\sqrt{x^2+\Delta z^2}}, \qquad (2)$$

where $i = \sqrt{-1}$, k is the angular wavenumber and $H_1^{(2)}$ is the Hankel function of the second kind and first order. (The f_n and Δz arguments have been dropped for brevity.)

Wave-field continuation by convolution can be interpreted with a simple physical model. Consider a point source embedded in a homogeneous medium and an array of geophones on a recording surface. When the source produces an acoustic emission, the wave field radiates outwards and is detected by the geophones. The portion of the wave field received at a particular geophone is determined by the spatial wavelet. Thus, the spatial wavelet can be regarded as a weighting function that governs the distribution of the wave field due to a point source (Figure 1a). This corresponds to the well-known exploding-reflector model of common-midpoint stacked data (Claerbout, 1985, p. 10). Alternatively, the spatial wavelet can weight the strength of many point sources and give the response at a particular geophone (Figure 1b). Determining the wave field at each receiver involves sliding the spatial wavelet over the collection of sources and summing up the source contributions according to the weighting function. Thus, convolution [equation (1)] computes the wave field on the recording surface by using linear combinations of the wave field on the source surface. The situation described above is for a single frequency. In reality, signals are composed of many frequencies, each requiring its own spatial wavelet for a single extrapolation step. In the space-frequency domain, a 1-D convolution is involved along the spatial (in this case x) axis for each component. Inverse Fourier transformation from the frequency domain to the time domain results in a zero-offset synthetic section. A schematic summary is shown in Figure 2.

Wave-field continuation can be done recursively or nonrecursively (Figure 3). The recursive approach is based on Huygen's principle where every point on an advancing wavefront can be considered as the source of a secondary wave and that a later wavefront is the envelope tangent to all the secondary waves. Consequently, the continuation procedure starts out with the original diffractor as an input which produces the radiated wave field. This output is in turn used as the input for the next extrapolation step. This process is repeated until the wave field has been upward-continued from the source surface to the recording surface. In contrast, the nonrecursive implementation uses a single

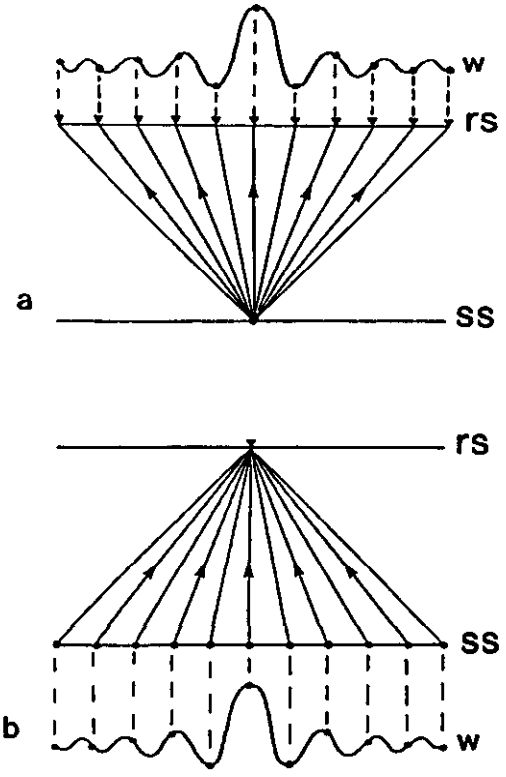

Fig. 1. Physical interpretation of spatial convolution. In both panels rs and ss indicate recording surface and source surface, respectively. (a) The wavelet W gives the response of a linear array of geophones to a point source. (b) The wavelet gives the value of the wave field at a single geophone due to a linear array of point sources.

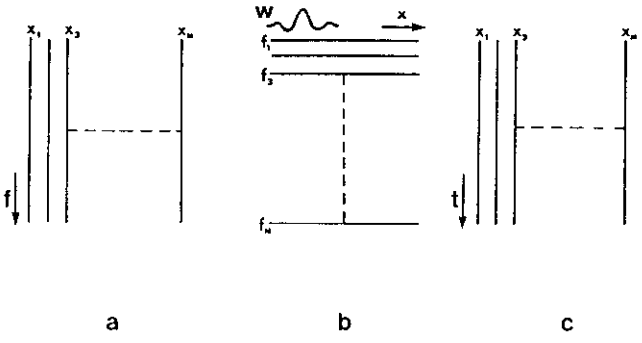

Fig. 2. Forward extrapolation in the (a) space-frequency domain involves (b) reordering from traces to frequency components and one-dimensional convolution along the x-axis for each frequency and (c) a one-dimensional inverse Fourier transform (frequency to time) to obtain the space-time section (after Berkhout, 1982). There are N frequences and M traces depicted.

step for extrapolating from source surface to recording surface. In a homogeneous medium the nonrecursive implementation can be used since no velocity changes occur. However, in cases where there are vertical and lateral inhomogeneities the recursive approach can be implemented to model the velocity variations. Figure 4 shows the difference in using the two schemes for a homogeneous medium. The model is a point source located at the centre of the spread at a depth of 500 m. The trace spacing was

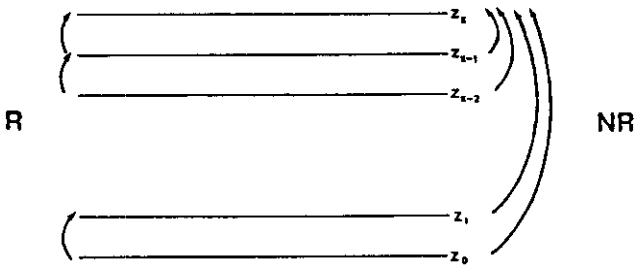

Fig. 3. Schematic diagram of recursive (R) versus nonrecursive (NR) wave-field continuation. Recursive implementation uses the output of the previous step as the input for the next step and requires k steps for the complete extrapolation. Nonrecursive implementation also requires k steps but each depth level is extrapolated to the surface in a single step. Nonrecursive extrapolation cannot accommodate vertical and lateral velocity changes.

$\Delta x = 25$ m, the velocity was $v = 4000$ m/s and the frequency band was 10-40 Hz. Figures 4a and 4b show the nonrecursive and recursive examples, respectively. The nonrecursive example uses a single extrapolation step of 500 m, whereas the recursive case uses ten steps of 50 m each. The results are virtually identical (a desirable result) except

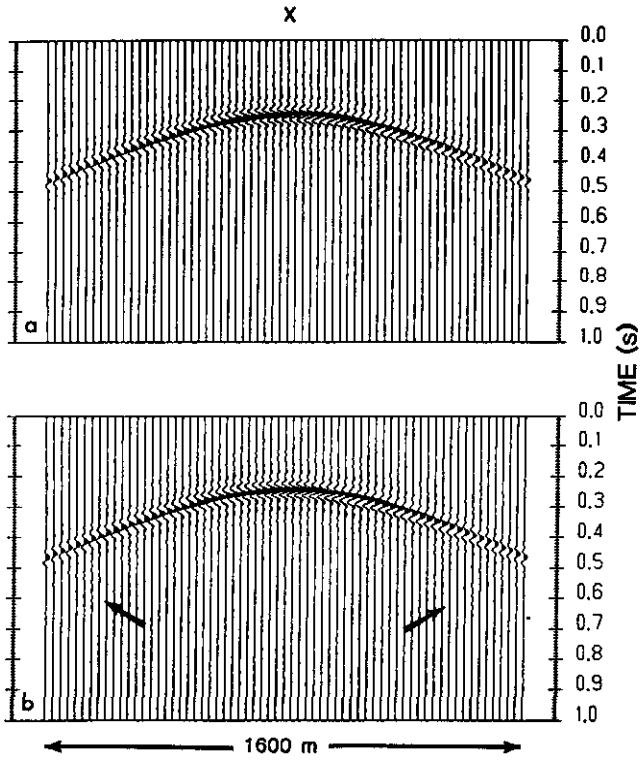

Fig. 4. Sections computed for a homogeneous medium. The examples demonstrate the difference in using (a) nonrecursive and (b) recursive extrapolation. Arrows indicate diffraction tails reflected from the data boundary. The extrapolation step sizes were 500 m and 50 m for (a) and (b), respectively. The frequency band was 10-40 Hz, the trace spacing was 25 m and the velocity was 4000 m/s.

for the very weak diffraction tails in the recursive implementation. This is due to the fact that in the recursive method the extrapolated wave field is "reflected" from the data boundary. The artifact is seen better by viewing the section at an angle in the directions of the arrows. The fact that there are a finite number of traces and a finite number of samples in what should be an infinite spatial wavelet leads to the artifact. For the point diffractor, only the first extrapolation step in the recursion is exact. All subsequent steps are slightly inaccurate because the wave field at the edge of the traces ends abruptly. This causes the wave field near the edges to act as a set of diffractors whose diffraction tails are not cancelled by neighbouring diffractor responses.

In this paper, the application of scalar diffraction theory for one-way wave propagation to reflection seismology has some important limitations (e.g., Trorey, 1970) that must be kept in mind. Firstly, either compressional waves (P) or shear waves (S) can be modelled but not both. Since the results of most industrial surveys are P-wave sections, I consider only that wave field. Secondly, only the upcoming wave field is modelled and the exploding reflector model is invoked. Thirdly, transmission losses are considered negligible and can be ignored [although Berkhout (1982) discusses how to include these effects]. Fourthly, the velocity of the medium is considered constant. Fifthly, the theory works best in the short-wavelength or high-frequency limit where the scale of the structure to be modelled is greater than the largest wavelength used in the modelling; otherwise, the predictions deteriorate.

Examples

The numerical examples shown are not intended to be exhaustive or even representative of the detailed type of modelling that would be needed in reality. Rather, they serve to illustrate some basic results of the spatial convolution technique in velocity regimes of varying complexity. To the best of my knowledge, zero-offset modelling results using spatial convolution have not appeared before this in the literature.

Constant velocity: synform model

A constant-velocity acoustic medium is one in which only P-waves are considered and their propagation velocity is constant throughout the medium. Since seismic reflections arise from variations in acoustic impedance, this implies that only the density in the medium is changing. Although this is not a realistic model, it is useful as a tool for demonstrating the modelling procedure. Since the spatial wavelet is formulated for a constant-velocity medium, modelling implementation is straightforward and follows the ideas laid out in the previous section.

Consider a synform embedded in a constant-velocity ($v = 4000$ m/s) medium such that the depth of burial ($d = 500$ m) is greater than the radius of curvature ($r = 250$ m) of the synform (Figure 5a). The condition $d > r$ results in the bow-tie effect that is familiar to reflection seismologists. The synthetic section (Figure 5b) shows the bow-tie effect and correctly models the diffraction extending beyond the synform edges (edges pointed out by arrows). Due to the practical considerations of

implementation, such as wavelet antialiasing (Nautiyal, 1988) and truncation (Nautiyal, 1986, p. 65), the dip information is limited to approximately 30 to 35 degrees.

The quality of the spatial-wavelet modelling was examined by migrating the synthetic data with an independent method. For a constant-velocity medium, the Stolt (1978) migration algorithm is accurate and very fast. Figure 5c shows the traveltime image that should be formed by proper migration. The migrated data are shown in Figure 5d and they match the traveltime image very well. In addition, the diffractions due to the synform edges have been collapsed to show the sharp corners; and the temporal wavelets are zero-phase. The amplitudes of the steep dip portions of the synform are weak due to the limitations of the modelling algorithm.

Horizontally stratified velocities: synform model

A more realistic model of the velocity field is that of horizontally stratified layers. The velocity may vary with depth but is assumed to be laterally invariant, i.e., $v = v(z)$. This layered earth model is supported by the empirical work of Faust (1951) which showed that P-wave velocity varied with the burial depth and geologic age rather than with the reflection structure. Thus, the layered earth model can be a justifiable approximation to the true earth in many cases, and it allows for a preliminary analysis of the modelling scheme at a level of complexity greater than that of the constant-velocity case. The spatial wavelet formulation cannot accommodate continuously varying $v(z)$ and, in practice, discrete horizontal layers with constant velocities are treated. In each layer the constant-velocity formulation was used.

The synform model of the constant-velocity case is reconsidered with introduction of a velocity change through the synform, at a depth of 630 m (Figure 6a). The velocities above and below this depth are 2000 m/s and 4000 m/s, respectively. The seismic section (Figure 6b) shows that with the introduction of the velocity stratification the bow-tie effect has been lost. In its place is a result that might be interpreted as a synform with $d < r$. (When $d<r$ a synform appears as a synform.) Clearly, vertical variations in the velocity can have important implications on the observed reflection structure.

Again, the modelling quality was judged using the image recovered through migration. For the $v = v(z)$ case, Gazdag's (1978) phase-shift migration was used. The expected traveltime image is shown in Figure 6c. The kinks in the synform occur because the migration is in time rather than depth. In order to recover the synform a time-to-depth conversion is needed. Figure 6d shows the migrated data and indicates that the modelling performed very well but that it was limited to accommodating dips of 30 to 35 degrees as in the previous example. Again, the edges of the synform are correctly imaged.

Laterally varying velocities: Kjartansson's fault-plane model

A more complicated model employed is one in which the velocity may vary both vertically and laterally, i.e., $v = v(x, z)$. In this section, only lateral velocity variations, $v = v(x)$, are assumed. Berkhout and van Wulfften Palthe (1979) suggested using space-variant or adaptive spatial wavelets for waves propagating in media with laterally

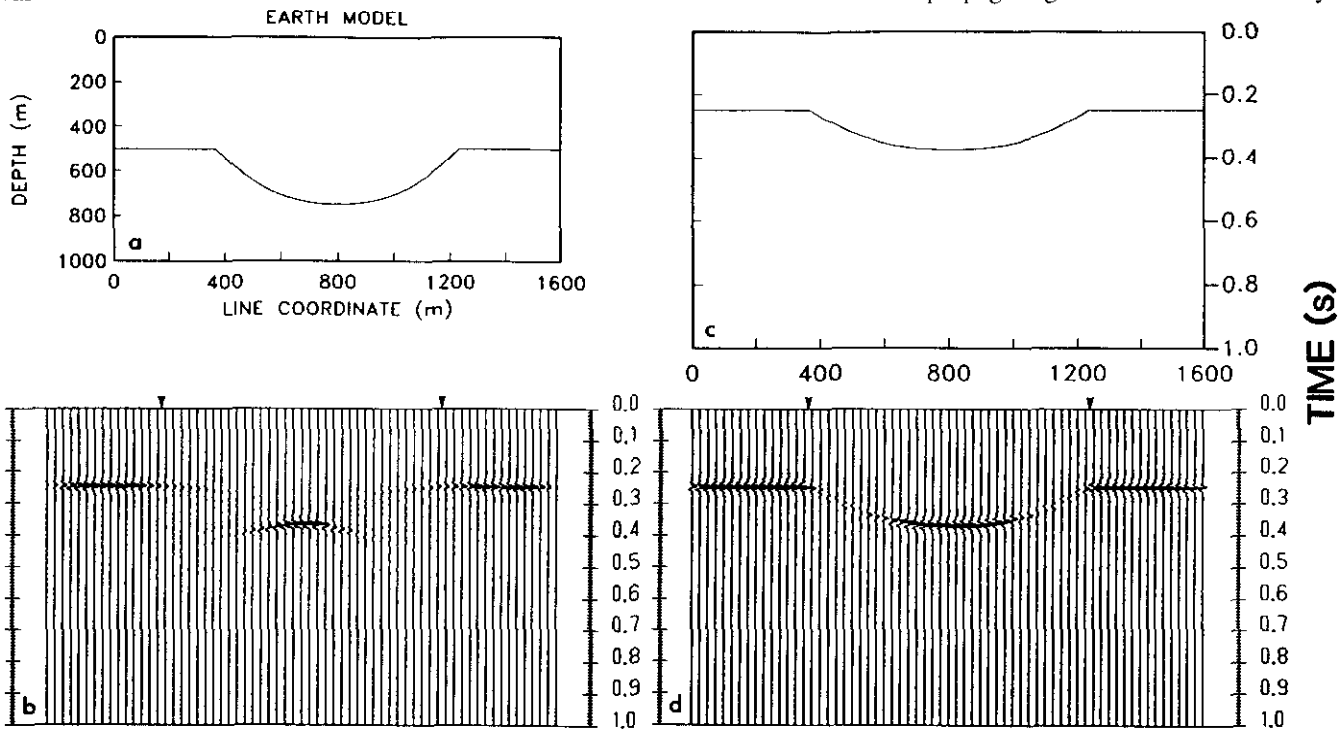

Fig. 5. Synform model with $d>r$ in a homogeneous medium: (a) earth model with constant velocity of 4000 m/s; (b) synthetic section for (a); (c) time-migration image line drawing; and (d) Stolt migration of synthetic data in (b). Arrows indicate positions of corner points in the model. Parameters are Δx = 25 m, Δz = 10 m and 10-80 Hz bandwidth.

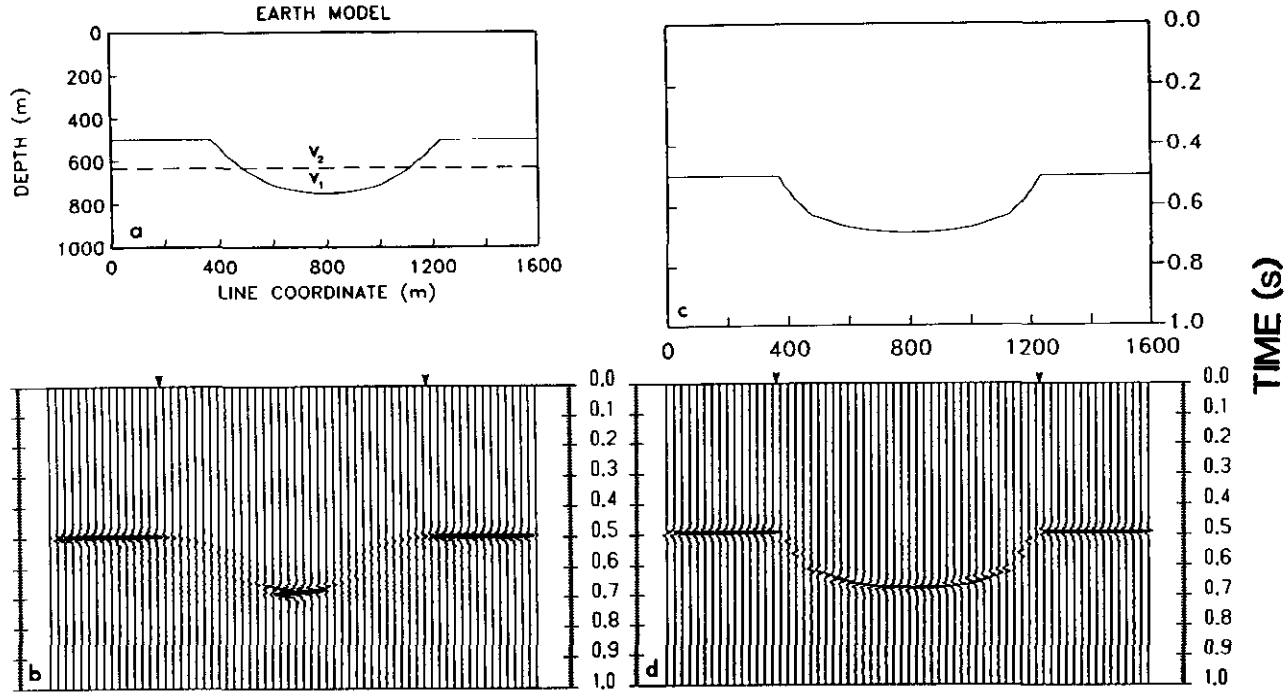

Fig. 6. Synform model with $d>r$ in a horizontally stratified medium: (a) earth model with velocities of v_1 = 4000 m/s and v_2 = 2000 m/s below and above the 630-m depth; (b) synthetic section for (a); (c) time-migration image line drawing; and (d) phase-shift migration of synthetic data in (b). Arrows indicate positions of corner points in the model. Parameters are Δx = 25 m, Δz = 10 m and 10-80 Hz bandwidth.

changing velocities, although they did not give details on how to do so. As in the horizontally stratified case, the constant-velocity spatial wavelet is inappropriate. However, I suggest that i) if the extrapolation step size is less than the shortest wavelength and ii) if the lateral velocity gradient (which has units of frequency, Hz) is lower than the low-end frequency used in the modelling, then adaptive convolution may be implemented with the constant-velocity spatial wavelet. The spatial wavelet changes according to the local lateral velocity. This approach should produce approximate results.

To study laterally varying velocity structures with adaptive spatial wavelets, Kjartansson's fault-plane model (Claerbout, 1985, p. 227, Figure 3.7-6) was used. This model consists of a point diffractor embedded in a velocity regime that varies only laterally. The model comprises two velocity zones (v_1 = 4000 m/s and v_2 = 5000 m/s) with the source located in the slower medium at a distance of 50 m from the boundary and at a depth of 500 m. Figure 7 shows a sketch of the types of waves generated by this configuration. The spatial-wavelet formulation cannot model the head wave (3) or the internally reflected wave (2), but it can model the direct wave (1) and the transmitted wave (4). Synthetic sections were computed using a frequency band of 10-40 Hz, a trace spacing of 25 m over an 800 m distance (the 33 centre traces in Figure 4) and an extrapolation increment of 10 m (the shortest wavelength was 100 m).

In Figures 8a and 8b the lateral velocity profile and the computed seismic section are shown, respectively. The velocity transition occurs over 25 m (the trace spacing) and this results in a lateral velocity gradient of 40 Hz. Since the frequency range used was 10-40 Hz, the spatial wavelet formulation cannot adequately describe the rapid velocity variation. This is shown in the generation of an artifact (arrow in Figure 8b). The results are similar to those shown by Claerbout (1985, p. 227, Figure 3.7-6), but direct comparison is impossible since Claerbout's parameters are not revealed.

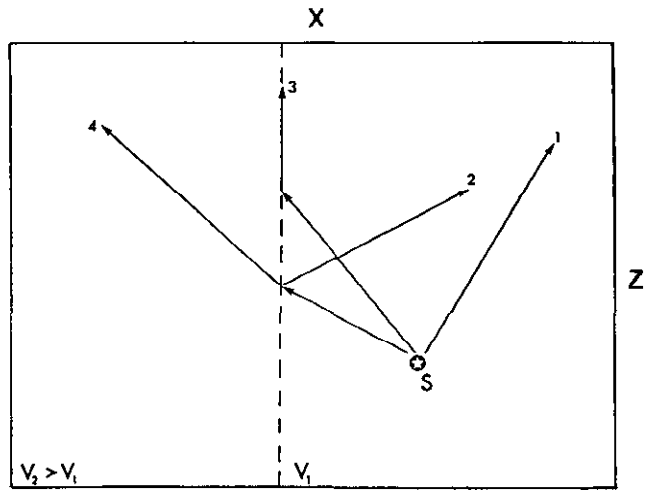

Fig. 7. Waves generated at a lateral velocity discontinuity. When the source (S) is in the slower medium four types of *P*-waves are expected: (1) the direct wave, (2) the internally reflected wave, (3) the head wave and (4) the transmitted wave. If the source were in the faster medium, wave type (3) would not be generated. The spatial wavelet method is able to describe only wave types (1) and (4).

The theory cannot handle the large velocity contrast over a small distance. A solution is to smooth the velocity gradient over a larger distance to guarantee a velocity gradient which is lower than the low-end of the modelling frequency band. Consequently, a smooth velocity profile was computed using an average weighted by an exponentially decaying function:

$$v_s(x_0) = \frac{\int_{-L}^{L} v(x)\, w_s(x_0 - x)\, dx}{\int_{-L}^{L} w_s(x_0 - x)\, dx}, \quad (3)$$

where $v_s(x_0)$ is the smoothed velocity function, $v(x)$ is the original velocity function, $w_s(x)$ is the weighting function and L is the length or aperture of the wavelet. The smoothing integral is over the aperture because that is the lateral extent to which the spatial wavelet is attempting to model wave propagation. The particular weighting function used is given by

$$w_s(x) = e^{-(x/\eta)^2}, \quad (4)$$

where η is the decay rate or smoothing factor. Small values of η (< 1) indicate fast decay and minimal smoothing, while large values ($\eta > 1$) express the opposite case. When $\eta = 0$ there is no smoothing.

The velocity profile with smoothing ($\eta = 3$) is shown in Figure 8c. The average velocity gradient is 2.6 Hz and the local maximum is 7.2 Hz (less than the low-end frequency of 10 Hz). The section in Figure 8d shows a smooth and continuous reflection signature with the artifact observed in Figure 8b being attenuated. Unfortunately, evaluation of the results was not possible due to software restrictions. However, it is clear that to satisfy theoretical constraints, model resolution has been sacrificed.

Conclusions

The spatial wavelet method for seismic reflection modelling provides a 1-D convolution approach to understanding wave propagation by wave-field continuation. After the basic concepts were reviewed, illustrative examples of the method for velocity models of varying complexity were provided. The modelled results for the constant and horizontally stratified cases were migrated to recover traveltime images using Stolt and phase-shift migrations, respectively. The migrated results matched the expected traveltime images very well and had characteristic zero-phase wavelets. This indicated that the modelling technique gave good synthetic sections. The data for the laterally varying velocity model were difficult to evaluate. The theory proved inadequate for general circumstances, and special conditions which smeared the model were required to make the theory applicable as an approximate method. Evaluation was not possible due to software restrictions and I welcome other solutions (e.g., physical or computer modelling, migrated result) to this model.

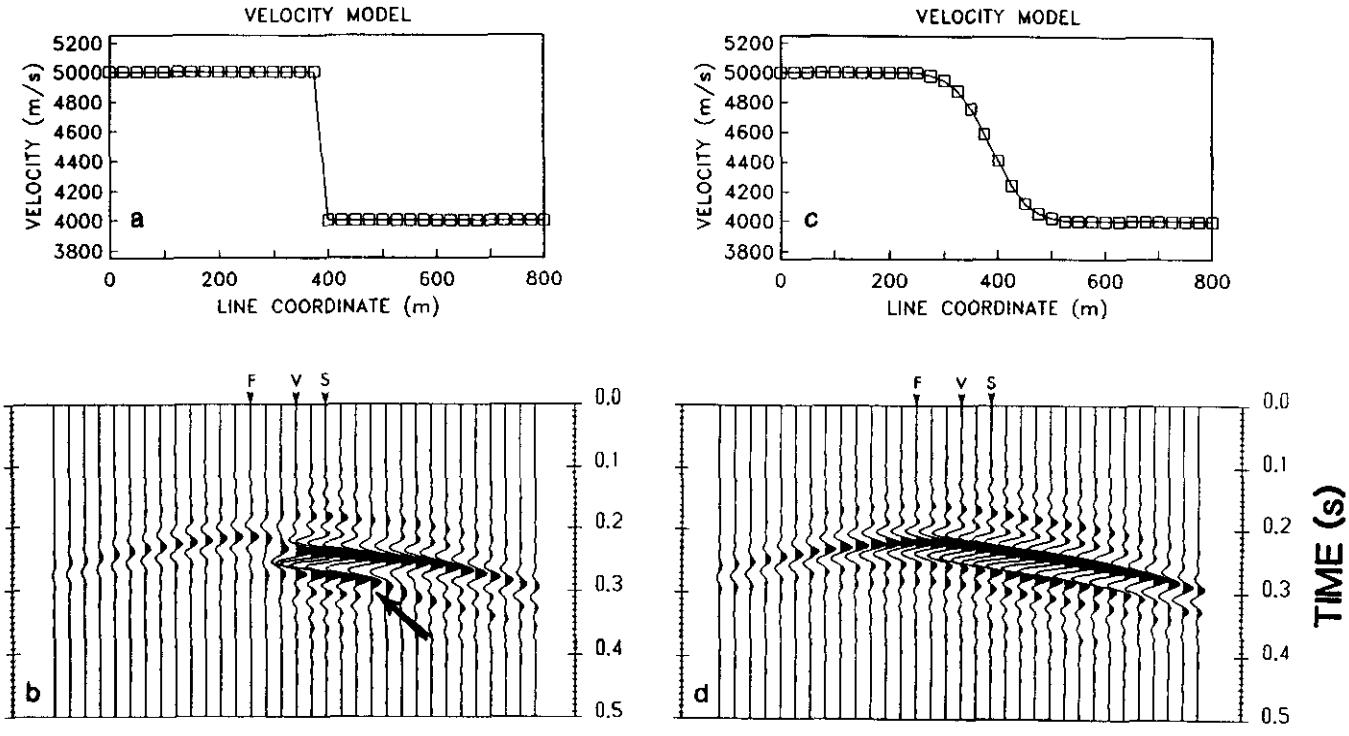

Fig. 8. Sections for a point source located near a lateral velocity discontinuity. On both synthetic sections, F, V and S indicate positions of first arrival, velocity boundary and source, respectively. The spread length on all sections is 800 m. Boxes in the velocity profiles indicate discrete velocities used in the calculations. (a) Lateral velocity profile without smoothing ($\eta = 0$). Maximum local velocity gradient is 40 Hz. (b) Synthetic section with $\eta = 0$. Arrow points to artifact generated due to lack of smoothing. (c) Lateral velocity profile with $\eta = 3$. Maximum local velocity gradient is 7.2 Hz. (d) Synthetic section with $\eta = 3$.

References

Berkhout, A.J., 1982, Seismic migration: A. Theoretical aspects: Elsevier Science Publ. Co., Inc.

_____ , 1984, Seismic migration: B. Practical aspects: Elsevier Science Publ. Co., Inc.

_____ and van Wulfften Palthe, D.W., 1979, Migration in terms of spatial deconvolution: Geophys. Prosp. **27**, 261-291.

Born, M. and Wolf, E., 1975, Principles of optics, 5th ed.: Pergamon Press, Inc.

Carter, J.A. and Frazer, L.N., 1983, A method for modeling reflection data from media with lateral velocity changes: J. Geophys. Res. **88**, 6469-6476.

Claerbout, J.F., 1985, Imaging the earth's interior: Blackwell Sci. Publ.

Faust, L.Y., 1951, Seismic velocity as a function of depth and geologic time: Geophysics **16**, 192-206.

Kelamis, P.G. and Kjartansson, E., 1985, Forward modeling in the frequency-space domain: Geophys. Prosp. **33**, 252-262.

Gazdag, J., 1978, Wave equation migration with the phase-shift method: Geophysics **43**, 1342-1351.

Kosloff, D.D. and Baysal, E., 1982, Forward modeling by a Fourier method: Geophysics **47**, 1402-1412.

Nautiyal, A., 1986, Aspects of spatial wavelets and their application to modelling seismic reflection data: M.Sc. thesis, Univ. of British Columbia.

_____ , 1988, Antialiasing methods for two-dimensional spatial wavelets in seismic modeling: Geophysics **53**, 1202-1206.

Shtivelman, V., 1985, Two-dimensional acoustic modeling by a hybrid method: Geophysics **50**, 1273-1284.

Stolt, R.H., 1978, Migration by Fourier transform: Geophysics **43**, 23-48.

Tieman, H.J., 1980, Modeling of the effects of lateral velocity variations on seismic data using the wave equation: J. Can. Soc. Expl. Geophys. **16**, 26-37.

Trorey, A.W., 1970, A simple theory for seismic diffractions: Geophysics **35**, 762-784.